Electrical Properties of $Gd_2Hf_{2-x}Zr_xO_7$ Solid Electrolytes Synthesized by Mechanical Milling

N.M. Cepeda-Sánchez[1], A.F. Fuentes[1], F.A. López-Cota[2], M. Rodríguez-Reyes[2] and J.A. Díaz-Guillén[2,*]

[1]Cinvestav Saltillo, Apartado Postal 663, 25000-Saltillo, Coahuila, México.
[2]División de Estudios de Posgrado e Investigación, Instituto Tecnológico de Saltillo, 25280-Saltillo, Coahuila México.
*Tel: +528444389539; e-mail: j.a.diazguillen@gmail.com

ABSTRACT

Gadolinium hafnates $Gd_2Hf_2O_7$ belong to a family of complex oxides with general formula $A_2B_2O_7$ which can show two different structural arrays, pyrochlore and non stoichiometric fluorite. These materials are known by their interesting electrical and thermal properties; thus, some of them are good oxygen ion conductors at high temperatures and can be used as solid electrolytes in SOFC's (Solid oxide Fuel Cells). Some others show low thermal conductivity and high thermal stability which make them attractive materials for TBCs (Thermal Barrier Coatings) to protect metal components of gas turbines and diesel engines.

The properties of these materials are significantly affected by the presence of defects such as vacancies and structural disorder. Therefore, their electrical and thermal properties can be modified by single or multiple chemical substitutions or by processing.

The ceramic method to obtain lanthanides hafnates usually involves thermal treatments at temperatures higher than 1500°C by long periods of time. This work deals with the mechanochemical synthesis and characterization of advanced ceramics of general formulae $Gd_2Hf_{2-x}Zr_xO_7$ (x = 0, 0.4, 0.8, 1.2, 1.6 and 2). This powder processing method allows obtaining metastable phases at room temperature that include a large number of structural defects, which will have an interesting effect on their electrical properties for their use as solid electrolytes. We also analyze the effect of substitution of Hf by Zr on the crystal structure and electrical properties of the gadolinium hafnate.

Results show that solid solutions $Gd_2Hf_{2-x}Zr_xO_7$ can be obtained by mechanical milling, by using a planetary mill and Yttria Stabilized Zirconia vials and balls. Their electrical properties, analyzed by impedance spectroscopy, reveal that these oxides are potential candidates to be used as solid electrolytes in SOFC's.

Keywords:SOFC's, pyrochlores, hafnates

1. Introduction

Solid Oxide Fuel Cells (SOFC´s) represent a highly efficient and environmentally friendly technology with a large variety of potential applications. Its operation is based on the combination of oxygen and hydrogen to produce electric energy and water. This technology is currently based on a combination of three active elements, a Sr-doped $LaMnO_3$ (LSM) cathode, 8YSZ solid electrolyte (yttria-stabilized zirconia with 8 mol% Y_2O_3) and a Ni-YSZ cermet anode. Unfortunately, cell performance is significantly affected by solid state reactions between components, which have been frequently observed during co-sintering or even during long-term operation at temperatures as low as 1000ºC. These reactions result in insulating phases, such as La_2Zr_2O7 and $SrZrO_3$, both having a detrimental effect on cell performance [1, 2]. Different possibilities to overcome this problem have been examined, such as using deficient La-site LSM perovskites for cathodes [3] or replacing La by some other lanthanides in LSM [4]. Alternative ceramic oxide-ion conductors have been also proposed to replace 8YSZ as solid electrolyte, among them $A_2B_2O_7$ oxides, such as $Gd_2Zr_2O_7$ and $Ln_2Hf_2O_7$ (Ln = Lanthanides), with the pyochlore-type structure [5,6]. These complex oxides represent an interesting group of solid ionic conductors because of their intrinsic concentration of oxygen vacancies (one vacancy by unit cell), their capacity to incorporate lanthanides and actinides in solid solution, their different degrees of structural order/disorder and stability at high temperatures [7].

Electroneutrality in these materials can be achieved by a large combination of cation species A and B (in $A_2B_2O_7$), with different oxidation states, and that is why their electrical behavior in pyrochlores varies widely. Thus, some pyrochlores such as $Gd_2Zr_2O_7$ represent the best pyrochlore-type oxygen ion conductors known, with σ_{dc} values similar to those of 8YSZ. On the other hand, pyrochlores as $Gd_2Mo_2O_7$ show at room temperature a metallic conducting behavior [7]. Different methods to obtain pyrochlores have been reported, such as solid state reaction at temperatures up to 1600ºC during long periods of time [8], co-precipitation [9], sol-gel [10], among others. Each method provides particular properties to the obtained powder.

Partial substitution of A and B ions for others in these materials can also have an effect on their properties. Some previous works reported the effect of partial substitution of Gd ion by different Lanthanides in the electrical properties of $Gd_2Zr_2O_7$ ([5, 11] and some other analyzed the properties of $Gd_2Ti_{2-x}Zr_xO7$ solid solutions [12]. In all cases results showed that solid solution can result in a increasing of ionic conductivity, one relevant property for solid electrolytes application, when the appropriate dopant elements are used.

In this context, and considering the importance of pyrochlores as solid electrolytes, this work studies the viability to obtain solid solutions of general formulae $Gd_2Hf_{2-x}Zr_xO7$ by mechanical milling, a powder processing method which has been successfully used by our group to prepare similar materials and that allows to obtain powders with high degree structural disorder.

Mechanical milling is a well known method to mechanically activate materials and to promote chemical reactions and alloying. This method has become a powerful powder processing method for the room temperature synthesis of a number of important multicomponent oxides (pyrochlores, fluorites and perovskites, to mention some). The obtained phases are frequently metastable, showing a large number of structural defects that are difficult to obtain by any other powder processing method. Contamination from the milling tools can be considered as a serious problem when hard and abrasive oxides are milled at high intensity for a prolonged time, but this problem can be substantially reduced by the appropriate selection of milling parameters [13].

We also evaluate, by impedance spectroscopy, the electrical properties of these ionically conducting materials. The changes of *dc* conductivity σ_{dc} and activation energy for ionic conduction E_{dc} are analyzed as a function of dopant content (x) in $Gd_2Hf_{2-x}Zr_xO_7$ series.
Considering the absence of reports on electrical properties of $Gd_2Hf_{2-x}Zr_xO_7$ system synthesized by mechanical milling, the results obtained in this study might be an important contribution to the scientific community.

2. Experimental

Five compositions of general formula $Gd_2Hf_{2-x}Zr_xO_7$ (x = 0-2) were prepared by mechanical milling starting from high purity (99.99%) Gd_2O_3, ZrO_2 and HfO_2. Starting chemicals were weighed out as required by stoichiometry, mixed and milled together in a planetary ball mill by using 125-ml zirconia containers with 20 mm diameter zirconia balls as to keep a ball-to-powder mass ratio of 10:1.
Mechanical milling was performed in air at room temperature by using a rotating disc speed of 350 rpm. Phase evolution on milling was analyzed by X-ray diffraction (XRD) in a Philips X'Pert diffractometer using Ni-filtered CuKα radiation (λ = 1.5418 Å). All reactions were considered complete when no traces of starting powders were identified by XRD. Electrical properties were measured from 280 to 750°C, on sintered pellets (10 mm diameter and ~1mm thickness) obtained by uniaxial pressing of the powders prepared by mechanical milling. In order to increase their mechanical strength and obtain dense samples, pellets were sintered at 1500°C for 12 hours (heating and cooling rate = 2°C/min). Analysis of electrical properties was carried out in air by Impedance Spectroscopy using a Solartron 1260 Frequency Response Analyzer over the 100 Hz-1MHz frequency range. Electrodes were made by coating both sides of the pellets with conductive platinum paint and firing them at 600°C to eliminate organic components and harden the Pt coating.

3. Results and discussion

Fig 1(a) shows an XRD study of the evolution, as a function of milling time, of the $Gd_2O_3 + ZrO_2 + HfO_2$ mixture, weighted in the appropriate proportion to obtain the composition $Gd_2Hf_{0.4}Zr_{1.6}O_7$, considered as representative of all five samples. XRD patterns correspond to the starting mixture and samples milled during 1, 3, 6, 9, 20 and 30 hours. As a reference, Fig 1(b) shows the XRD pattern reported in the International Centre for Diffraction Data, ICDD (PDF 80-0471) for the fluorite structure of $Gd_2Zr_2O_7$.
An important decrease in intensity and broadening of the characteristic reflections of starting oxides are observed after the first hour of milling, as a consequence of a considerable decrease in particle size and the introduction of a large number of structural defects. After 6 hours of milling, XRD patterns do not show appreciable changes, only a light decreasing of intensity of the main peaks.
After 9 hours, the powder mixture shows a pattern where the main reflections of the cubic anion deficient fluorite (e.g. (100), (200), (220) and (311)) can be appreciated. As the patterns of samples milled during 20 and 30 hours shows, further milling produces a significant increase in their intensities. Growth of the crystallites initially formed of this phase or the increment in their number with milling time, could be responsible for this effect. No additional phases seem to be present in the powder so reactions were considered completed after 30 hours of milling.
This behaviour is presented by all five studied compositions of the $Gd_2Hf_{2-x}Zr_xO_7$ system, such as Fig 2 shows.

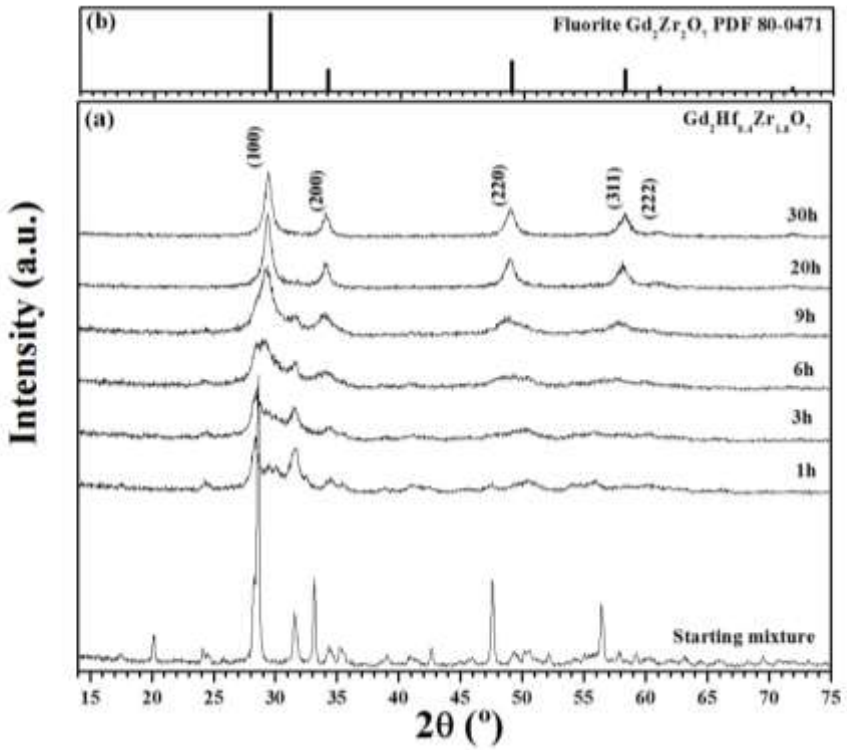

Fig 1. X-ray powder diffraction patterns showing the evolution of the composition $Gd_2Hf_{0.4}Zr_{1.6}O_7$ as a function of milling time (a). X-ray pattern of the fluorite-type $Gd_2Zr_2O_7$ reported in the ICDD (PDF 80-0471) (b).

Most of $A_2B_2O_7$ are known to exist in two crystal forms, as a highly disordered pyrochlores and as anion deficient fluorites [14]. The fully ordered ideal pyrochlore crystal structure exhibits cubic symmetry (S.G.: Fd3m) and can be regarded as an ordered anion deficient fluorite (cubic, S.G.: Fm3m) with twice the cell constant (see reference [7] for a complete description of the pyrochlore structure). The pyrochlore stability field at room temperature and atmospheric pressure in zirconates and titanates is limited to the $1.46 \leq R_A/R_B \leq 1.78$ range [15], corresponding values for $Gd_2Zr_2O_7$ (R_A/R_B for $Gd_2Zr_2O_7$ = R_{Gd}/R_{Zr} = 1.053 Å/0.72 Å = 1.46) [16], and $Sm_2Ti_2O_7$, respectively, and for anion-deficient fluorites R_A/R_B value should be less than 1.46). For the $Gd_2Hf_{2-x}Zr_xO_7$ system studied in this work, R_A/R_B ratio is in the range of 1.48 (for $Gd_2Hf_2O_7$) to 1.46 (for $Gd_2Zr_2O_7$), considering a R_{Hf} of 0.71 Å [16]. According to this ratio, all compositions analyzed in this work should present a pyrochlore type structure and degree of structural disorder will increase lightly with increasing of Zr (x) content (decreasing R_A/R_B).

Fig 2(a) shows a comparison between XRD patterns obtained for all studied compositions after milling for 30 hours as described above. As a reference, Fig 1(b) and (c) show the XRD patterns reported in the ICDD for the fluorite structure of $Gd_2Zr_2O_7$ (PDF 80-0471) and $Hf_2Zr_2O_7$ (PDF 24-0425) respectively. As Fig 2(a) shows, irrespective of their Zr-content and the R_A/R_B value, milled powders present simple and very

similar XRD patterns which resemble the characteristic of a fluorite-type compound, with no evidence of the reflections characterizing the long range atomic ordering of the pyrochlore crystal structure.
These results reveal that, as a far-from-equilibrium processing method, mechanical milling allows the preparation of metastable phases and defect structures existing at equilibrium only at high temperature and/or high pressure. Defect fluorites showing significant stability at elevated temperatures have been also prepared by mechanical milling in the $Gd_2(Ti_{1-y}Zr_y)_2O_7$ and $GdLaZr_2O_7$ system, for compositions with R_A/R_B values well above 1.46 [11,12] and that seems to be also the case in the $Gd_2Hf_{2-x}Zr_xO_7$ system where R_A/R_B changes from 1.46 to 1.48.

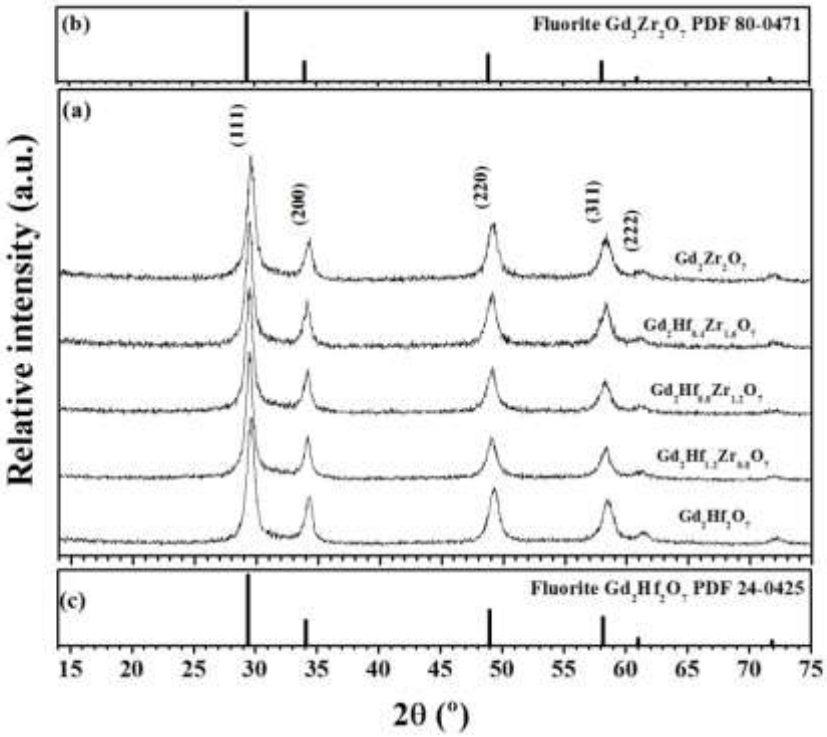

Fig 2. XRD patterns of five compositions of the $Gd_2Hf_{2-x}Zr_xO_7$ system after milling 30 hours (a). XRD patterns reported in the ICDD for the fluorite structure of $Gd_2Zr_2O_7$ (PDF 80-0471) (b) and $Hf_2Zr_2O_7$ (PDF 24-0425) (c).

Postmilling thermal treatments of these metastable powders, facilitates the rearrangement of the cation and anion substructures and the partial relaxation of mechanochemically induced defects in these materials.
This behaviour is showed in Fig 3 (a), which present the XRD patterns of all studied samples milled during 30 hours and fired at 1500°C for 12 hours. All samples fired present the superstructure reflections characterizing the pyrochlore crystal structure (i.e. the (111), (311) and (331) peaks at 2θ ≈15, 28 and 37° respectively). No additional reflections belonging to other phases are observed. The absence of reflections shift towards low or high angles (2θ) is not evident since Zr (0.72 Å) and Hf (0.71 Å) are very similar in size and then the change in the cell size with increasing of Zr content in $Gd_2Hf_{2-x}Zr_xO_7$ might be small to be identified by XRD.

Fig 3(b) and (c) show the XRD patterns reported in the ICDD for the pyrochlore structure of $Gd_2Zr_2O_7$ (PDF 80-0469) and the fluorite structure of $Hf_2Zr_2O_7$ (PDF 24-0425) respectively. Fig 3 (d) show an insert with an enlargement of an area of the XRD patterns and exhibits clearly the presence of the (311) peak corresponding to pyrochlore superstructure.

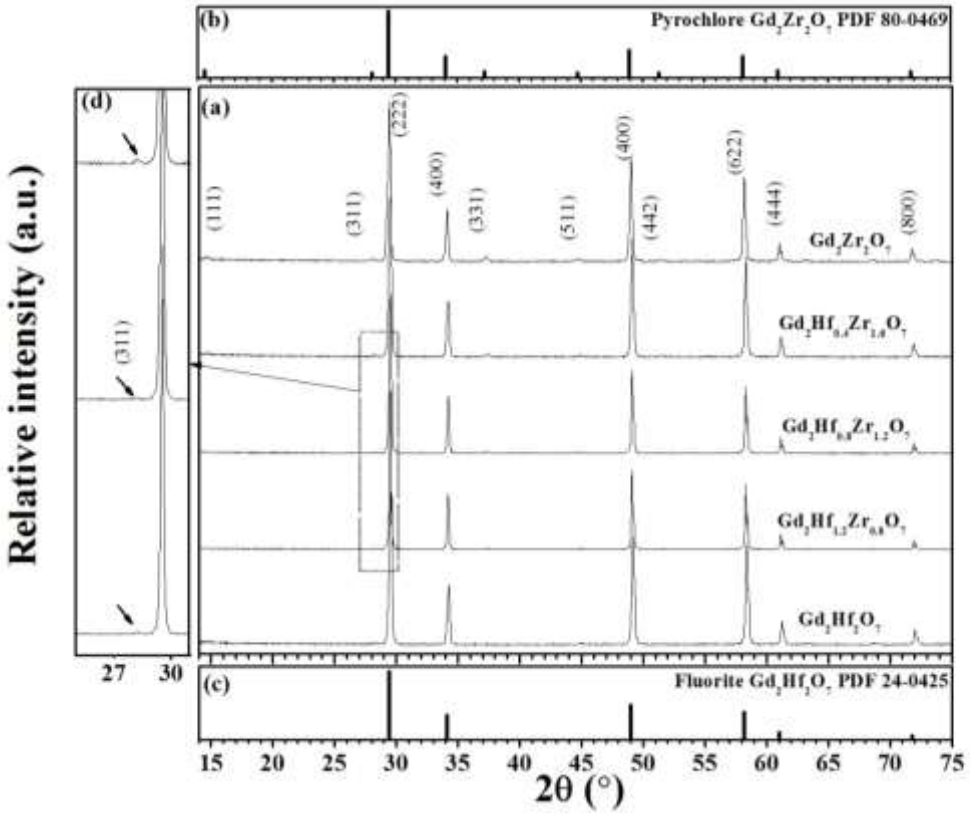

Fig 3. XRD patterns of $Gd_2Hf_{2-x}Zr_xO_7$ samples milled during 30 hours and fired at 1500°C for 12 hours (a). XRD patterns reported in the ICDD for the pyrochlore structure of $Gd_2Zr_2O_7$ (PDF 80-0469) (b) and fluorite structure of $Hf_2Zr_2O_7$ (PDF 24-0425) (c). Enlargement of XRD patterns showing the presence of the (311) peak of the pyrochlore superstructure (d).

The typical morphology of the unpolished $Gd_2Hf_{0.4}Zr_{1.6}O_7$ sample, milled during 30 hours and sinterized during 12 hours at 1500ºC is presented in Fig 4. It is clearly seen a microstructure with grains inhomogeneous and a grain size for less than 1 micrometer. Grain boundaries seem clean and no other phases are found at interfaces. Remanent porosity indicates that higher temperatures are necessaries to obtain totally dense samples. Similar behaviour was showed by all studied compositions.

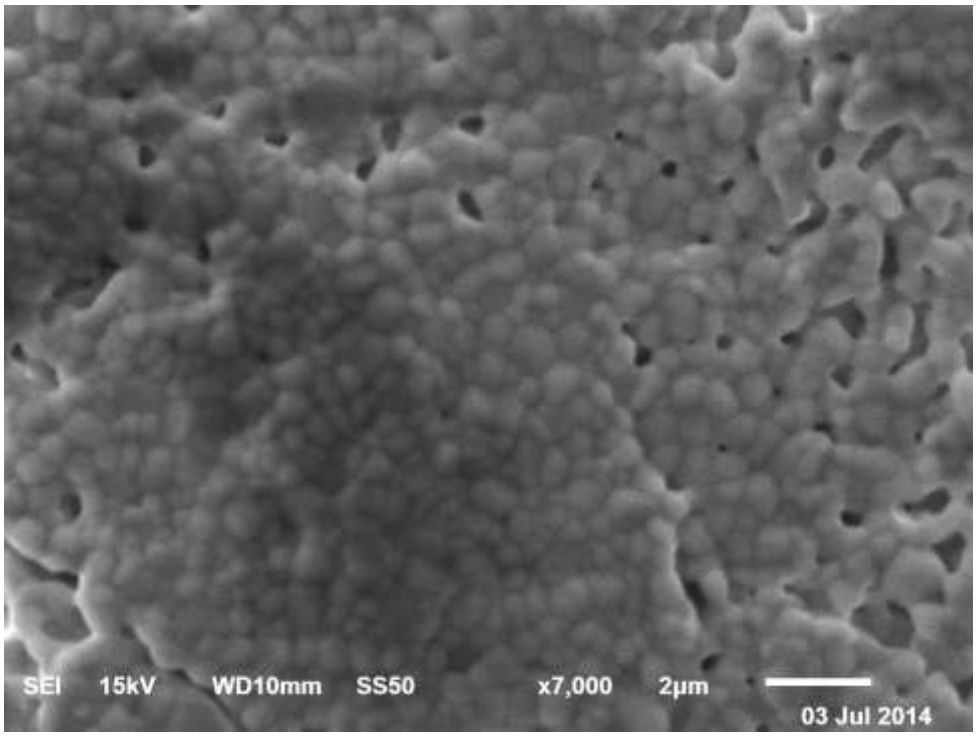

Fig 4. Morphology of the unpolished $Gd_2Hf_{0.4}Zr_{1.6}O_7$ sample, milled during 30 hours and sinterized 12 hours at 1500ºC, obtained by SEM (JEOL JSM 6610).

Fig 5 shows the frequency and temperature dependence of the real part of the electrical conductivity, σ'(ω), for the pyrochlore-type $Gd_2Hf_{0.4}Zr_{1.6}O_7$ sample selected as representative of the series. Similar conductivity plots were obtained for all samples analyzed in this work. As this Fig 5 shows, the frequency (ω) dependence of conductivity at low temperatures may be well described by the so-called Jonscher empirical expression , $\sigma'(\omega) \propto \omega^n$, consistent with a power law-type dependence at high frequencies followed by a frequency-independent conductivity plateau associated to the *dc* conductivity regime, σ_{dc}. This behavior constitutes the main feature of the so-called "Universal Dielectric Response" and has been linked with the existence of cooperative effects in the dynamics of hopping ions [17]. The value of the fractional exponent n ($0 \leq n < 1$) is determined by the strength of the ion-ion interactions in the ionic hopping process; i.e. in the absence of interactions among mobile ions (completely independent and random ion hopping), the exponent n would be 0. The decrease in conductivity clearly visible at low frequencies between 280 and 400°C is caused by blocking effects at grain boundaries whereas that observed at 750°C is due to blocking at the electrodes.
Fig 6 shows the real part of the electrical permittivity as a function of frequency and temperature for the same composition in a log-log representation. Blocking effects at grain boundaries and electrodes, which are characteristic of a charge transport dominated by the contribution of hopping ions, are evident in this graph and also points to the ionic nature of the electrical conductivity in these materials.

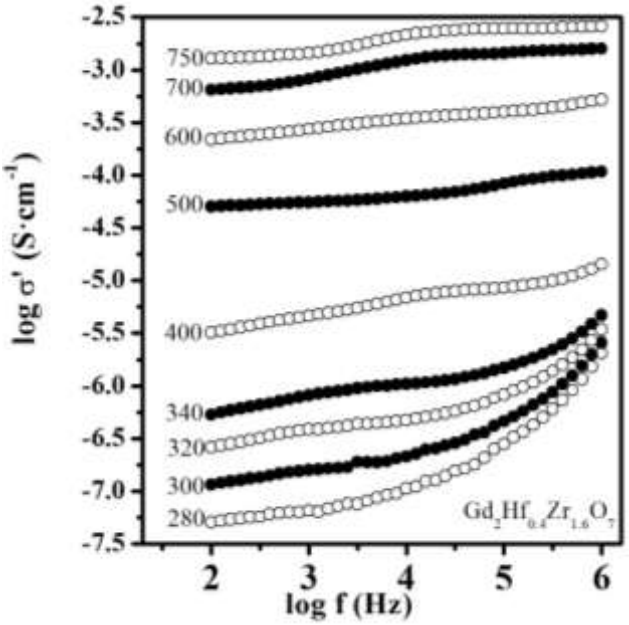

Fig 5. Real part of the conductivity vs frequency at several temperatures (°C) for the $Gd_2Hf_{0.4}Zr_{1.6}O_7$ composition showing a power-law behavior at high frequencies and low temperatures.

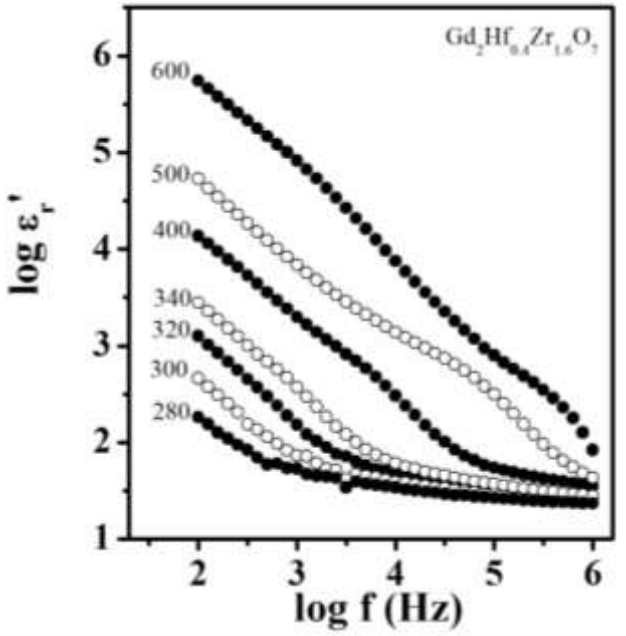

Fig 6. Frequency dependence of the real part of permittivity of $Gd_2Hf_{0.4}Zr_{1.6}O_7$, at selected temperatures (°C).

The temperature dependence of the *dc* conductivity for the samples under study was analyzed by using an Arrhenius-type law of the form:

$$\sigma_{dc} T = (\sigma_0) \exp(-E_{dc}/k_B T) \quad (1)$$

where σ_0 is the pre-exponential factor which is related to the effective number of mobile oxygen ions and E_{dc} denotes the activation energy for the ion conduction process. Fig 7 shows such representation for a selected sample, where the line is the least squares best fit to an Arrhenius law confirming that ionic diffusion in the series is thermally activated. Activation energies E_{dc} for the whole series were calculated from the slope of these linear fits.

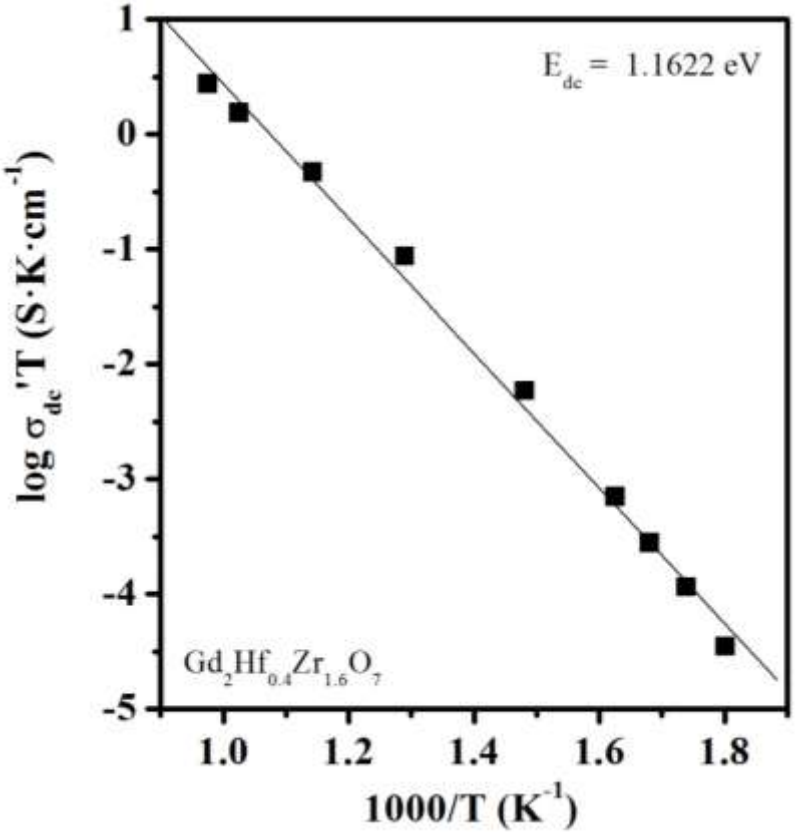

Fig 7. Arrhenius plot of the dc conductivity for the $Gd_2Hf_{0.4}Zr_{1.6}O_7$ composition. Solid line is the best fits to the experimental data.

Finally, Fig 8. shows *dc* conductivity activation energy E_{dc} and the *dc* conductivity σ_{dc} at 750ºC on Zr as a function of Zr content (x) for all the compositions of the system $Gd_2Hf_{2-x}Zr_xO_7$. An increasing of E_{dc} is evident with increasing of Zr content, in the interval of 0.87 to 1.17 eV. This behaviour suggests that incorporation of Zr (decreasing R_A/R_B) in the lattice of $Gd_2Hf_2O_7$ generates an increasing of structural

disorder and therefore an increment of the number of charge-carrier ions, which will contribute to the ionic conductivity. This will generate a higher correlation or interaction between mobile ions and will result in an increasing of the activation energy for *dc* conductivity.
However, the resulting *dc* conductivity shows an increment with increasing of Zr content, reaching a maximum for x = 1.6 and then decreases. Results show that σ_{dc} is a compromise between the increase in the number of carriers (higher disorder) and the activation energy E_{dc}, so that there is an optimum degree of disorder for which the highest *dc* conductivity is obtained.
These results showed that the most disordered material not always has the highest conductivity and the maximum is obtained for the 1.6 would represent precisely the optimal degree of disorder in the system $Gd_2Hf_{2-x}Zr_xO_7$.

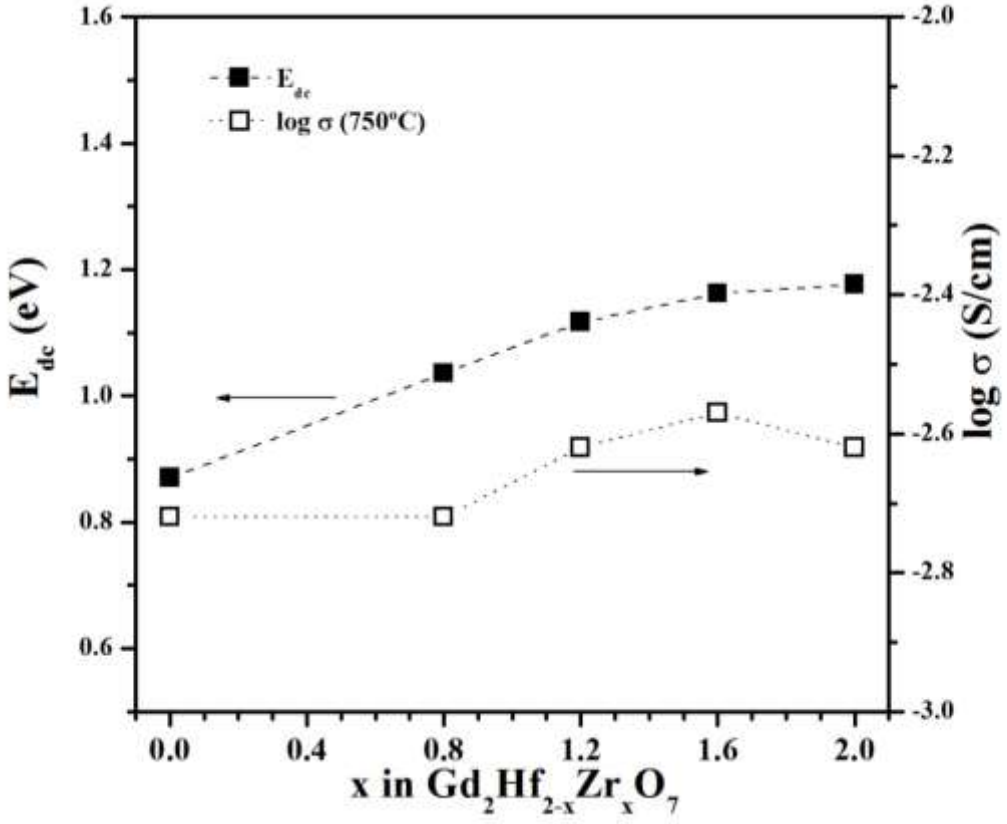

Fig 7. Dependence of the *dc* conductivity activation energy E_{dc} and the *dc* conductivity σ_{dc} at 750ºC on Zr content (x) for the system $Gd_2Hf_{2-x}Zr_xO_7$.

4. Summary and perspectives

We have shown that compositions in the $Gd_2Hf_{2-x}Zr_xO_7$ system having different Hf/Zr ratios can be easily prepared at room temperature by mechanically milling stoichiometric mixtures of the corresponding elemental oxides. As-prepared powder samples show XRD patterns similar to those characteristic of highly disordered anion-deficient fluorites, while postmilling thermal treatments at 1500ºC give rise to a partial redistribution of cations and oxygen vacancies and the appearance of the long-range atomic ordering characteristic of pyrochlores for all studied samples. Activation energy for migration increases as disordering increases (Zr content) and *dc* conductivity in the series reaches a maximum for x = 1.6 at 750ºC. This degree of doping would represent precisely the optimal degree of disorder in the system $Gd_2Hf_{2-x}Zr_xO_7$ to obtain the higher ionic conductivity.
Complex oxides of the general formula $Gd_2Hf_{2-x}Zr_xO_7$ represent an interesting group of ionic conductors that can be used as solid electrolytes in SOFC's technology.

Acknowledgements

This work has been carried out with the financial support of Mexican DGEST and CONACYT.

References

[1] J.A. Labrincha, J.R. Frade, F.M. Marques, $La_2Zr_2O_7$ formed at ceramic electrode / YSZ contacts. Journalof Materials Science 1993; 28: 3809-3815.
[2] A. Mitterdorfer, L.J. Gauckler, $La_2Zr_2O_7$ formation between yttria stabilized zirconia and $La_{0.85}Sr_{0.15}MnO_3$ at 1773 K. Journal of Solid State Chemistry of Inorganic Materials 1997; 453: 425-430.
[3] H. Yokokawa, N. Sakai, T. Kawada and M. Dokiya, Thermodynamic analysis of reaction profiles between $LaMO_3$ (M = Ni , Co , Mn) and ZrO_2. J. Electrochem. Soc 1991; 138: 2719-2727.
[4] Y. Takeda, Y. Sakaki, H-Y Tu, M. B. Phillipps, N. Imanishi and O. Yamamoto, Perovskite oxides for the cathode in solid oxide fuel cells. Electrochemistry 2000; 68: 764-770.
[5] J.A. Díaz-Guillén, A.F. Fuentes, M.R. Díaz-Guillén, J.M. Almanza, J. Santamaría, C. León, The effect of homovalent A-site substitutions on the ionic conductivity of pyrochlore-type $Gd_2Zr_2O_7$. Journal of Power Sources 2009: 186: 349–352.
[6] A.V. Shlyakhtina, L.G. Shcherbakova, Polymorphism and high-temperature conductivity of $Ln_2M_2O_7$ (Ln=Sm─Lu; M=Ti, Zr, Hf) pyrochlores. Solid State Ionics 2011; 192: 200–204.
[7] M.A. Subramanian, G. Aravamudan, G.V. Subba Rao, Oxide pyrochlore, A review. Progress in Solid State Chemistry 1985; 15: 55-143.
[8] B.P. Mandal, Nandini Garg1, Surinder M. Sharma1, A.K. Tyagi, Preparation, XRD and raman spectroscopic studies on new compounds $RE_2Hf_2O_7$ (RE = Dy, Ho, Er, Tm, Lu, Y): Pyrochlores or defect-fluorite. Journal of Solid State Chemistry 2006; 179: 1990–1994.
[9] Z.G. Liu, J.H. Ouyang, Y. Zhou, X.L. Xia, Coprecipitation synthesis and sintering property of $(Yb_xSm_{1-x})_2Zr_2O_7$ ceramic powders. Advances in Applied Ceramics 2010; 109: 12-17.
[10] B. Vijaya Kumara, Radha Velchuria, G. Prasadb, B. Sreedharc, K. Ravikumard, M. Vithala, Preparation, characterization, photoactivity and XPS studies of Ln_2ZrTiO_7 (Ln = Sm and Nd). Ceramics International 2010; 36, 4: 1347–1355.
[11] J.A. Díaz-Guillén, M.R. Díaz-Guillén, J.M. Almanza, A.F. Fuentes, J. Santamaría, C. León, Effect of La substitution for Gd in the ionic conductivity and oxygen dynamics of fluorite-type $Gd_2Zr_2O_7$. Journal of Physics: Condensed Matter 2007; 19: 356212.
[12] K.J. Moreno, G. Mendoza, A.F. Fuentes, J. García-Barriocanal, C. León, J. Santamaría, Cooperative oxygen dynamics in fuel cell materials $Gd_2Ti_{2-y}Zr_yO_7$. Physical Review B 2005; 71: 132301.
[13] A.F. Fuentes; L. Takacs , Preparation of multicomponent oxides by mechanochemical methods. Journal of Materials Science 2013; 48, 2: 598-611.
[14] M.P. van Dijk, A.J. Burggraaf, A.N. Cormack, C.R.A. Catlow, Defect structures and migration mechanisms in oxide pyrochlores. Solid State Ionics 1985; 17: 159-167.
[15] P.K. Moon, H.L. Tuller, Fast ion conduction in the $Gd_2(Zr_xTi_{1-x})_2O_7$ pyrochlore system. Mater. Res. Soc. Proc. 1989;135: 149-155.
[16] R.D. Shannon, Revised effective ionic radii and systematic studies of interatomic distances in halides and chalcogenides. Acta Crystalografica A32 1976; 751-767.
[17] A.K. Jonscher, Dielectric relaxation in solids, Chelsea Dielectric London 1983.